Type of contribution:
Editorial
▶ Research Paper
Case Study
Review Paper
Scientific Data
Report of Tech. Application

e-issn. 2798-5245
Mechanical Engineering for Society and Industry
Vol. 6, No. 2 (2026) pp 350-361
https://doi.org/10.31603/mesi.14926

Influence of oil palm frond fiber loading on the morphological, mechanical, and acoustic properties of polyurethane composite foams

Budi istana[1]*, Adriyan[1], Agus Mulyadi[2], Cici Maarasyid[3], Jeefferie Abd Razak[4]

[1] Department of Mechanical Engineering, Universitas Muhammadiyah Riau, Pekanbaru 28294, **Indonesia**
[2] Department of Industrial Engineering, Universitas Muhammadiyah Riau, Pekanbaru 28294, **Indonesia**
[3] Department of Chemical Engineering, Universitas Muhammadiyah Riau, Pekanbaru 28294, **Indonesia**
[4] Fakulti Teknologi dan Kejuruteraan Industri dan Pembuatan, Universiti Teknikal Malaysia Melaka, Hang Tuah Jaya, 76100 Durian Tunggal, Melaka, **Malaysia**

✉ budiistana@umri.ac.id

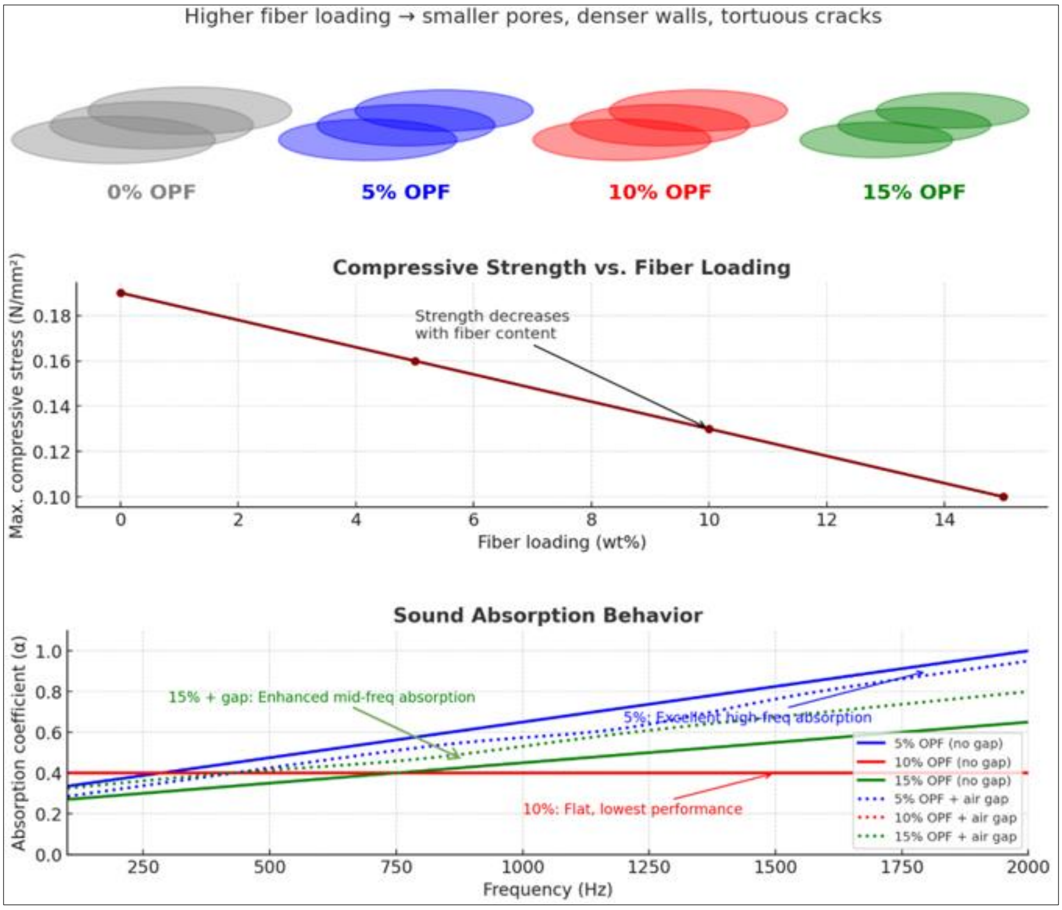

Highlights:

- Oil palm frond (OPF) fibers were incorporated into polyurethane composite foams.
- OPF loading significantly modified foam cell morphology and pore distribution.
- Mechanical strength showed a moderate reduction with increasing OPF content.
- OPF–PUF composites exhibited enhanced acoustic absorption at mid–high frequencies.
- Findings highlight OPF fibers as sustainable reinforcement for multifunctional foams.

Article info
Submitted: 2025-09-29
Revised: 2026-07-04
Accepted: 2026-07-19

Publisher
Universitas Muhammadiyah Magelang

Abstract

The development of sustainable acoustic materials is increasingly important for reducing environmental impact while maintaining functional performance. In this study, rigid polyurethane (PU) foams reinforced with oil palm frond (OPF) fibers were fabricated with fiber loadings of 0, 5, 10, and 15 wt% to investigate the structure–property–performance relationship. Morphological characterization by SEM revealed that increasing fiber content refined pore size from ~539–742 µm in neat PU to ~224–663 µm at 15 wt% OPF, with higher tortuosity and evidence of fiber pull-out. Mechanical testing showed that maximum compressive stress decreased systematically with fiber addition (0.19 N/mm² in neat PU to 0.10 N/mm² at 15 wt%), reflecting increased slurry viscosity, fiber agglomeration, and imperfect interfacial adhesion. Acoustic measurements demonstrated that 5 wt% OPF provided superior high-frequency absorption (α ≈ 0.95 at 2000 Hz), while 10 wt% OPF consistently underperformed due to pore blockage. At 15 wt%, absorption became more stable across mid-to-high frequencies (0.35–0.60), and when combined with a 10 mm air gap, the composites exhibited enhanced broadband performance, particularly between 400–1600 Hz. These results establish a clear link between fiber loading, cell morphology, compressive strength, and acoustic behavior. Low fiber contents are best suited for hybrid strength–acoustic applications, while higher loadings combined with cavity backing offer an eco-friendly route to broadband sound absorbers. The findings highlight OPF fibers as a promising renewable reinforcement for multifunctional PU foams in building and automotive insulation.

Keywords: Polyurethane foam composites; Oil palm frond (OPF) fiber; Bio-based acoustic materials; Sound absorption coefficient; Air gap acoustic enhancement

1. Introduction

Polyurethane foams (PUFs) are widely used in automotive [1], construction [2], and industrial applications [3] because of their light weight, thermal insulation, and ease of processing [4]. However, conventional PUFs face critical challenges. They are derived from petroleum resources, raising sustainability concerns, and they often exhibit poor durability at elevated temperatures [5], [6]. More importantly, their sound absorption capability, particularly at low and mid frequencies, is limited. These shortcomings restrict their effectiveness in noise control applications, where materials are expected to deliver broad-frequency absorption while maintaining structural integrity.

Over the past two decades, researchers have explored numerous approaches to improve the properties of polyurethane foams. Inorganic fillers such as alumina, silica, and metal oxides have been added to increase thermal resistance [5], while synthetic fibers and mineral reinforcements have been used to enhance mechanical strength [2]. More recently, attention has shifted toward natural fibers such as jute, kenaf, coir, sisal, and hemp. These fibers have demonstrated potential to reinforce polymer foams, alter pore morphology, and improve interfacial adhesion [6], [7]. Several studies report that natural fiber reinforcement can reduce thermal conductivity, increase char yield during degradation, and provide moderate improvements in mechanical strength [3], [8]. Despite these efforts, the acoustic potential of natural fiber–reinforced polyurethane foams has not been explored as thoroughly as their structural and thermal behaviors [4].

Although natural fibers are increasingly studied in composites, oil palm biomass, particularly oil palm frond (OPF) fibers, has received little attention in the context of polyurethane foams. This is surprising given the abundance of OPF as an agricultural byproduct in Southeast Asia, where millions of tons are discarded annually. Existing research has focused more on oil palm empty fruit bunches (EFB) and shells, while OPF fibers remain underutilized. Furthermore, most studies have emphasized mechanical and thermal characteristics, overlooking systematic investigations into acoustic performance. In particular, the combined effect of fiber-induced morphological changes and simple acoustic enhancement strategies such as backing air gaps has rarely been studied in OPF–PUF systems.

To address this overlooked area, the present study proposes the incorporation of OPF fibers into rigid polyurethane foams as a sustainable reinforcement strategy proposes the incorporation of OPF fibers into rigid polyurethane foams as a sustainable reinforcement strategy for acoustic functionality. The concept is that OPF fibers will alter pore size distribution, increase airflow resistivity, and introduce microstructural heterogeneity that promotes viscous and scattering losses of sound energy. Additionally, an air gap of 10 mm is introduced behind the composite samples during testing to investigate cavity resonance effects, which are known to enhance low-frequency absorption. to investigate cavity resonance effects, which are known to shift the absorption spectrum toward lower frequency bands. By combining fiber reinforcement with cavity-backed configurations, this study aims to develop a simple yet effective pathway to broaden the absorption spectrum of bio-based foams.

The primary goal of this research is to establish clear structure–property relationships in OPF–PUF composites. Specifically, the work examines how OPF content influences morphology and mechanical strength, and thermal stability, and how these changes translate into acoustic performance with and without an air gap. By correlating SEM microstructural observations with functional outcomes, the study seeks to demonstrate that OPF fibers can be used not only to improve sustainability but also to significantly enhance the acoustic insulation properties of polyurethane foams.

This work contributes to both scientific understanding and practical application. From a scientific perspective, it addresses a clear research gap in the acoustic behavior of natural fiber–reinforced foams, particularly those based on OPF. From a practical standpoint, it highlights an underutilized biomass resource as a reinforcement that could reduce environmental waste while delivering multifunctional performance. The findings are expected to benefit the design of eco-friendly acoustic panels for buildings, automotive interiors, and industrial insulation, where lightweight, sustainable, and broadband noise-control materials are increasingly demanded.

2. Methods

2.1. Material

The OPF utilized in this study was sourced from oil palm trees that were approximately 10-15 years old. Following the pruning process, fronds were collected and subjected to a series of preparatory steps to convert them into suitable bio-fiber reinforcement. Oil palm fronds (OPF) were collected from a plantation in Kampar Regency, Riau Province, Indonesia. The fronds were cleaned, dried, and mechanically chipped to obtain chips with an average thickness of 5–10 mm. Polyurethane foam (PUF) was synthesized from commercial-grade polyol and methylene diphenyl diisocyanate (MDI) supplied by Sutindo Chemical Group, mixed at a 1:1 weight ratio. All chemicals were used without further purification.

2.2. Fiber Preparation

The OPF fibers were washed thoroughly to remove surface impurities, dried at 80 °C for 24 h, milled and sieved to obtain a particle size distribution corresponding to 60 mesh (~250 µm), as shown in **Figure 1**. Prior to composite fabrication, the fibers were oven-dried at 105 °C for 2 h to ensure moisture content below 10 wt%.

Figure 1. Oil palm frond fiber: (a) Plant; (b) Palm Fronds; (c) OPF chips; (d) OPF fiber

2.3. Fabrication of OPF-PUF Composites

Polyurethane foams reinforced with varying OPF fiber loadings (0, 5, 10, and 15 wt%) were prepared using a free-rise foaming process. Prepolymer foams were produced using a conventional one-shot process. Component A—comprising catalyst, propylene glycol, surfactant, and deionized water—was premixed, after which liquid MDI was incorporated at a 1:1 mass ratio with the polyol to form rigid foams of moderate density. For composites, OPF fibers were dry-mixed into the polyol before adding the isocyanate and stirring at 1000 rpm for 8 s. The mixtures were then cast into box molds, allowed to rise freely, and annealed at 70 °C for 30 min, and conditioned at 22 °C and 50% relative humidity for 24 h before demolding [9]. After two weeks, the samples were cut and tested, as schematically illustrated in **Figure 2**.

2.4. Characterization

2.4.1. Morphology

The cellular structure of the foams was examined using a Field Emission Scanning Electron Microscope (FESEM, Hitachi SU5000). Prior to observation, specimens were sputter-coated with a thin layer of gold–palladium using a Quorum sputter coater to enhance surface conductivity.

Imaging was conducted at an accelerating voltage of 10 kV with magnifications in the range of 50–100×. The obtained micrographs were analyzed to evaluate foam cell size, pore distribution, and the dispersion of OPF fibers within the polyurethane matrix.

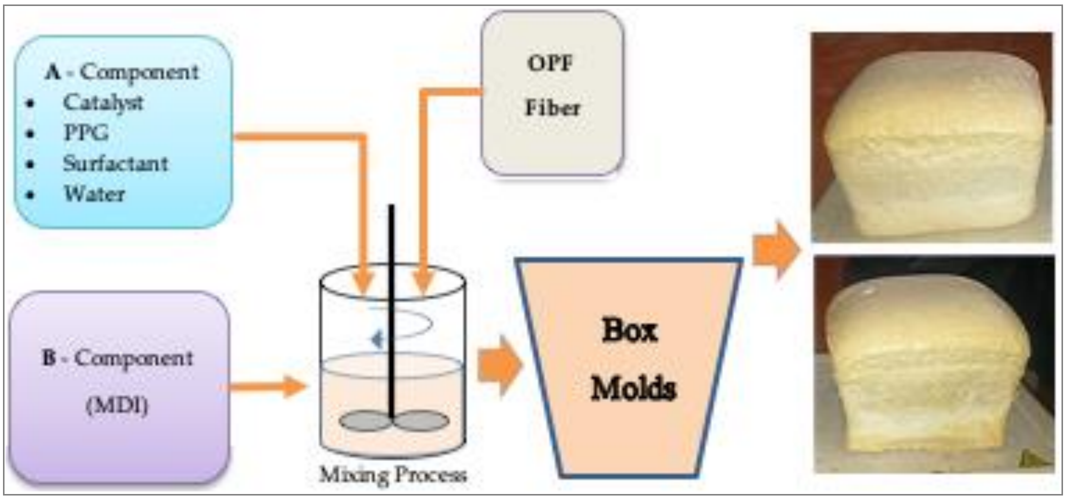

Figure 2. The synthesis process of bio-fiber based PU composites

2.4.2. Mechanical properties

Compressive strength tests were performed using a Shimadzu Autograph universal testing machine with a maximum load capacity of 20 kN (**Figure 3a**). The procedure followed ASTM D1621, ensuring consistency with standardized methods for rigid cellular plastics and enhancing the reliability of the reported data. To ensure statistical significance and data reproducibility, three replicates (*n*=3) were tested for each fiber loading (0, 5, 10, and 15 wt% OPF). Prismatic specimens (**Figure 3b** to **Figure 3d**) with dimensions of 50 × 50 × 26 mm were carefully prepared and inspected to verify thickness uniformity prior to testing. The specimen geometry is critical, as it influences load distribution and ensures representative mechanical behavior. A constant crosshead speed of 0.26 mm/s was applied until specimen failure, and the maximum load was recorded for compressive strength determination.

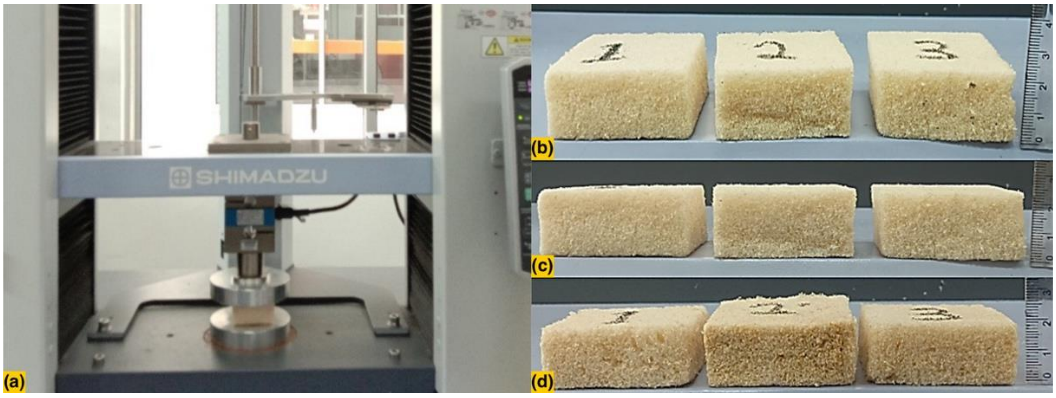

Figure 3. Photographs of selected specimens following compressive strength testing: (a) Shimadzu Autograph 20 kN universal testing machine; (b) Neat PU; (c) 5% OPF; (d) 15% OPF

2.4.3. Acoustic properties

The sound absorption coefficient was measured using a two-microphone impedance tube system (BSWA, MPA416, 1/4-inch). Two tube setups (**Figure 4**) enabled measurements across 50–2000 Hz. Disk specimens (20 mm thick, 33 mm diameter) were prepared following ISO 10534-2 and ASTM E1050 (**Figure 5**).

Measurements were conducted under two configurations: (i) direct placement of the specimen against the rigid backing and (ii) placement with a 10 mm air gap between the specimen and the backing surface to evaluate the cavity effect on low-frequency absorption. placement with a 10 mm air gap between the specimen and the backing surf-

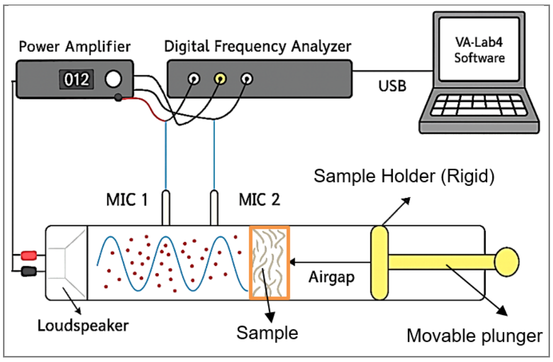

Figure 4. Laboratory measurement setup for sound absorption coefficient measurement

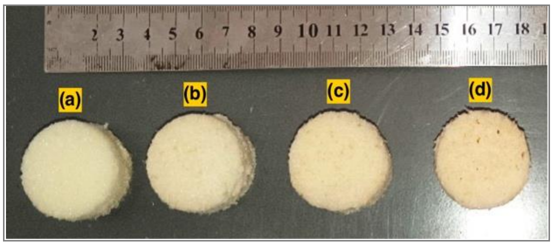

Figure 5. Samples prepared for sound absorption test: (a) Neat PU; (b) 5% OPF; (c) 10% OPF; (d) 15% OPF

ace to evaluate the cavity effect in shifting the absorption peaks toward lower frequencies. Data from the low- and high-frequency tubes were merged into a single continuous curve using VA-Lab software (BSWA), yielding frequency-dependent absorption plots for each configuration. The introduction of an air gap is known to shift the peak absorption towards lower frequencies; therefore, comparative results with and without the air gap were analyzed. The noise reduction coefficient (NRC) was calculated as the arithmetic mean of absorption at 250, 500, 1000, and 2000 Hz for both configurations. NRC distills the frequency-dependent absorption curve into a single, dimensionless value.

While the acoustic behavior of the composites was evaluated using the two-microphone impedance tube system, direct measurements of airflow resistivity and absolute porosity were not conducted. Instead, these parameters were qualitatively inferred by correlating the physical sound absorption coefficients with the quantitative morphological data obtained via SEM analysis.
The noise reduction coefficient (NRC) was calculated by Eq. (1).

$$NRC = \frac{\alpha 250 + \alpha 500 + \alpha 1000 + \alpha 2000}{4} \tag{1}$$

The notation α250, α500, α1000, and α2000 refers to the sound absorption coefficients measured at 250, 500, 1000, and 2000 hertz, respectively. Each α value conveys how much acoustic energy a given medium retains at its matching frequency.

3. Results and Discussion

3.1. Morphological Analysis

The fractured morphology of the neat PU foam (0 wt% OPF) exhibits relatively large and irregular cells, with diameters ranging from 539 to 742 µm exhibited an average cell size of 640.5 µm, with a distribution range of 539–742 µm. The cell walls appear thin and brittle, producing flat fracture surfaces with minimal tortuosity. Such structural features are consistent with poor crack resistance and low toughness, as cracks can easily propagate across thin ligaments without significant deflection. Similar observations have been reported in unfilled PU foams, where large cell sizes and thin walls correlate with brittle failure behavior and lower compressive strength. For instance, Ölcay *et al*. [10] measured large average cell sizes in pure PU foams and showed that those with large pores have lower sound absorption coefficients and reduced mechanical performance.

The addition of 5 wt% OPF fibers markedly alters the foam architecture, producing a more heterogeneous cell size distribution (418–897 µm). Upon adding 5 wt% OPF, the mean cell size shifted to 657.5 µm, reflecting a more heterogeneous structure as fibers acted as nucleation sites. While some larger pores persist, the emergence of smaller cells suggests that the fibers act as nucleation sites during expansion, interrupting bubble coalescence and promoting finer structures. The fractured surfaces at this loading appear noticeably rougher, with clear signs of fiber pull-out and matrix tearing, features that point to enhanced energy dissipation compared to the neat PU. This behavior can be linked to mechanisms such as fiber bridging and crack deflection, as well as the increase in slurry viscosity caused by fiber incorporation, which together suppress uncontrolled cell growth. Comparable observations have been reported in other natural fiber–reinforced PU systems, including henequen and cellulose fiber foams, where low fiber additions (typically 1–5 wt%) refined the pore network, increased crack tortuosity, and translated into measurable gains in compressive modulus and energy absorption [10], [11].

At 15 wt% OPF loading, the cell structure becomes significantly refined, with average diameters reduced to 224–663 µm and noticeably thicker walls. At the highest loading of 15 wt% OPF, the mean cell size significantly decreased to 443.5 µm, confirming that higher fiber content and increased slurry viscosity effectively limit bubble growth and refine the pore network. The significant refinement of the pore network at 15 wt% OPF loading (224–663 µm compared to 539–742 µm in neat PU) and the appearance of noticeably thicker cell walls provide a structural proxy for increased airflow resistivity. The highly tortuous crack paths observed in the fractured morphology suggest a more complex internal geometry, which is theoretically associated with increased tortuosity and enhanced viscous losses during acoustic wave propagation. This densification reflects the combined effect of higher slurry viscosity and fiber-induced nucleation, which limit bubble growth and coalescence. The fractured morphology shows highly tortuous crack paths, consistent with improved fracture resistance. These results align with earlier work by Murmu *et al*. [12], where renewable natural fiber content in PU foams reduced the average cell sizes to under ~400 µm and produced enhancements in mechanical and thermal behavior.

The higher magnification micrograph (**Figure 6d**) provides critical insight into the fiber-matrix interaction. highlights the fiber-matrix interaction. The OPF fibers are partially embedded in the PU matrix, with clear evidence of fiber pull-out and matrix tearing. with evidence of pull-out and resin coating along the fiber surfaces. This morphology suggests partial interfacial adhesion imperfect interfacial adhesion, characterized by a combination of mechanical interlocking and debonding where both mechanical interlocking and debonding coexist. Because the hydrophilic OPF fibers were used in their untreated state, their compatibility with the hydrophobic PU matrix is limited, which ultimately restricts the efficiency of stress transfer across the interface. While fiber pull-out contributes positively to energy absorption, weak adhesion can limit stress transfer efficiency. Prior studies have shown that surface treatments like alkali-silane modifications significantly enhance fiber-matrix bonding, reducing pull-out and shifting fracture behavior toward cohesive failure within the matrix.

Importantly, these microstructural changes also have implications for acoustic performance. Smaller and more tortuous pores as observed at higher OPF loadings are known to increase viscous and thermal losses in open-cell foams, thereby improving mid to high frequency sound absorption. Studies by Yang *et al*. [13] and Lazzari *et al*. [14] demonstrate that refining pore size, increasing tortuosity, and enhancing interconnected porosity correlate strongly with enhanced sound absorption coefficients in natural-fiber composite panels and PU foams alike.

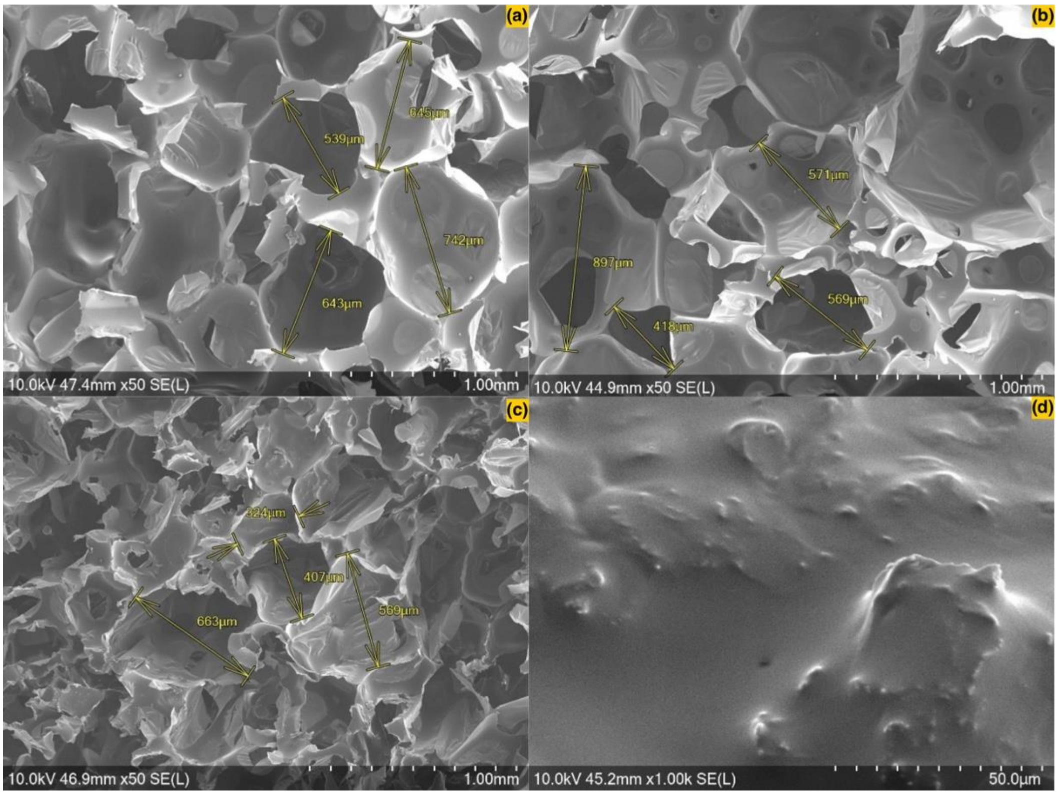

Figure 6. Fractured morphology and cell size distribution of: (a) 0 wt%; (b) 5 wt%; (c) 15 wt%; (d) Fiber matrix interaction

3.2. Mechanical Properties

To clarify the primary drivers of mechanical performance, the bulk density of the PU/OPF composites was evaluated alongside compressive strength (**Table 1**). While all samples were synthesized to maintain a moderate density, the results reveal a systematic decline in compressive stress from 0.1901 N/mm² (neat PU) to 0.0941 N/mm² (15 wt% OPF). The compressive strength of the PU/OPF composites shows a steady decline as fiber content increases, dropping from 0.1901 N/mm² in the neat foam to 0.094 N/mm² at 15 wt% OPF. This downward slope (–0.0064 N/mm² per %OPF) reflects a systematic reduction in load-bearing capacity with each increment of fiber addition. The steady decline in compressive strength (from 0.19 to 0.094 N/mm²) is directly influenced by the quality of the internal interface. While fibers can act as nucleating agents, the lack of optimized interfacial bonding between the hydrophilic fibers and hydrophobic matrix causes the fibers to act as structural defects rather than reinforcements. The presence of fiber pull-out under compressive loads confirms that the polymer network, rather than the fiber reinforcement, dominates the load-bearing behavior, as the weak interface fails to facilitate effective stress distribution.

The relatively small error bars, representing the standard deviation across three replicates (*n*=3), indicate reproducible behavior across replicates, underscoring that the trend is inherent to the composite structure rather than experimental scatter. Similar reductions have been reported in other natural fiber–reinforced polyurethane foams, where excessive fiber content raises slurry viscosity, promotes agglomeration, and disrupts cell-wall integrity, ultimately weakening compressive resistance [10], [12]. While small amounts of fiber can act as nucleating agents and improve local stiffness, beyond a threshold the reinforcing effect is offset by structural discontinuities and poor interfacial adhesion, leading to the observed decline in compressive strength [11], [15].

Several studies on polyurethane foams reinforced with natural fibers report similar reductions in compressive strength with higher filler loadings. For example, Ölcay *et al*. [10] found that natural fillers increased heterogeneity in pore structure, lowering compressive strength beyond 10 wt% content. Likewise, Murmu *et al*. [12] observed that renewable natural fiber–reinforced PU foams showed strength enhancement only at very low loading, with higher fractions leading to reduced wall integrity and premature failure. Comparable results were documented by Kovuru *et al*. [16] in composites reinforced with sisal and hemp fibers, where compressive strength decreased due to stress concentrations at poorly bonded fiber–matrix interfaces.

While the maximum compressive stress decreased systematically from 0.19 N/mm² to 0.094 N/mm², the OPF fibers effectively 'reinforced' the acoustic energy dissipation pathways (**Figure 7**). As shown in the morphological analysis, fiber addition refined the pore size from ~539–742 µm to ~224–663 µm and increased crack tortuosity. Therefore, while the fibers act as a structural diluent that weakens the load-bearing capacity due to increased slurry viscosity and imperfect interfacial adhesion, they simultaneously function as a morphological modifier that enhances sound absorption performance. The reduction in compressive strength can be attributed to three main mechanisms. First, high fiber loading increases slurry viscosity, impeding uniform foam expansion and promoting irregular cell formation, as shown in our SEM analysis (large heterogeneity at 5 wt% and smaller, denser but brittle cells at 15 wt%). Second, lignocellulosic fibers tend to agglomerate at higher concentrations, forming defects that act as crack initiation sites. Third, interfacial bonding between hydrophilic OPF fibers and the hydrophobic PU matrix is not fully optimized, leading to fiber pull-out under compressive loads. Studies by Andersons *et al*. [11] and Kuranchie *et al*. [17] confirm that weak fiber–matrix adhesion limits stress transfer, with compressive stress dominated by the polymer network rather than reinforcement.

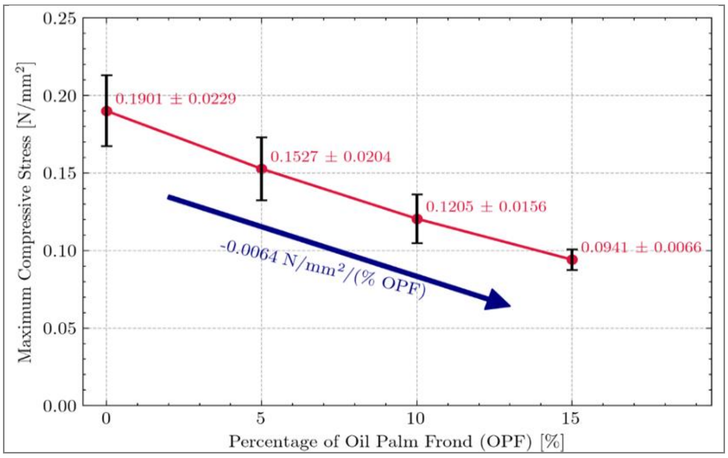

Figure 7. The compressive stress of the PU/OPF composites

Table 1. Physical and mechanical properties of OPF-PU composite foams

Sample Code	OPF Fiber Loading (wt%)	Bulk Density (kg/m^3)*	Max. Compressive Stress (N/mm^2)	n
Neat PU	0	0.0483	0.1901 ± [0.0229]	3
PU/OPF 5%	5	0.0393	0.1527 ± [0.0204]	3
PU/OPF 10%	10	0.0377	0.1205 ± [0.0156]	3
PU/OPF 15%	15	0.0340	0.0941 ± [0.0066]	3

3.3. Acoustic Properties

The sound absorption behavior of the PU/OPF composites demonstrates a strong dependence on both fiber loading and air gap configuration. Without an air gap, the neat PU exhibits modest absorption, with values rising gradually toward high frequencies and reaching ~0.75 at 2000 Hz. This is typical of open-cell PU foams, which are more effective in the upper frequency range due to increased viscous and thermal losses in smaller pores [5], [10], [18], [19]. The addition of 5 wt% OPF markedly enhances high-frequency absorption, achieving nearly 0.95 at 2000 Hz, indicating that fiber incorporation increases airflow resistivity and improves energy dissipation. The addition of 5 wt% OPF achieved a high-frequency absorption of nearly 0.95 at 2000 Hz, a result attributed to inferred increases in airflow resistivity driven by fiber-induced structural heterogeneity. Although specific resistivity values were not measured, the observed 'pore blockage' and reduced permeability at 10 wt% offer functional evidence that fiber loading directly alters the flow resistance of the open-cell network, thereby dictating the dissipation of acoustic energy [20]. Similar enhancements have been reported for kenaf and rice plant reinforced PU foams, where fibers` disrupted cell uniformity and increased tortuosity, thereby promoting viscous damping [10], [13], [21].

Interestingly, the 10 wt% OPF composite displays flatter absorption performance, with coefficients between 0.35–0.45 across the measured spectrum. Previous studies show that when fiber content exceeds the threshold for uniform dispersion, pore blockage and reduced permeability occur, leading to diminished acoustic efficiency [11], [12]. In contrast, the 15 wt% OPF sample achieves a more balanced response, with coefficients between 0.35–0.60 and gradual improvement above 1000 Hz. This behavior can be linked to fiber agglomeration and disrupted open-cell connectivity, as also reflected in its SEM morphology. This suggests that although higher fiber contents reduce compressive strength, they stabilize airflow resistivity, providing a favorable compromise between structural morphology and absorption capability [22], [23], [24], [25].

The introduction of a 10 mm air gap substantially alters absorption performance, particularly at low to mid frequencies (**Figure 8b**). For neat PU, absorption remains poor, confirming that the improvements arise primarily from fiber reinforcement. With the air gap, the 5 wt% OPF composite shows a strong peak (~0.78 at 1000–1400 Hz), consistent with the resonance effect of the backing cavity that extends absorption into lower bands With the air gap, the 5 wt% OPF composite shows a strong peak (~0.78 at 1000–1400 Hz), which is consistent with the resonance effect of the backing cavity that enhances mid-frequency absorption and shifts the peak toward lower bands compared to the samples without a gap [13], [26], [27]. By contrast, the 10 wt% OPF composite again underperforms, remaining flat between 0.3–0.45, underscoring the detrimental effect of agglomerated fibers. The 15 wt% OPF composite, however, benefits substantially, with absorption values of 0.45–0.60 across 400–1600 Hz. This performance reflects the synergy between fiber-induced resistivity and cavity-induced resonance, a phenomenon also reported in natural fiber nonwovens and PU–EFB composites [28].

The NRC values further confirm these trends (**Figure 9**). Without an air gap, values ranged from 0.35 to 0.45, with the 5 wt% and 15 wt% composites slightly outperforming neat PU. The 10 wt% composite recorded the lowest NRC (0.35), in line with its weaker frequency response. With a 10 mm air gap, NRC values improved modestly, with the 5 wt% and 15 wt% composites both reaching 0.50. This indicates that cavity backing not only shifts the absorption spectrum toward lower frequencies but also improves overall energy dissipation across the NRC

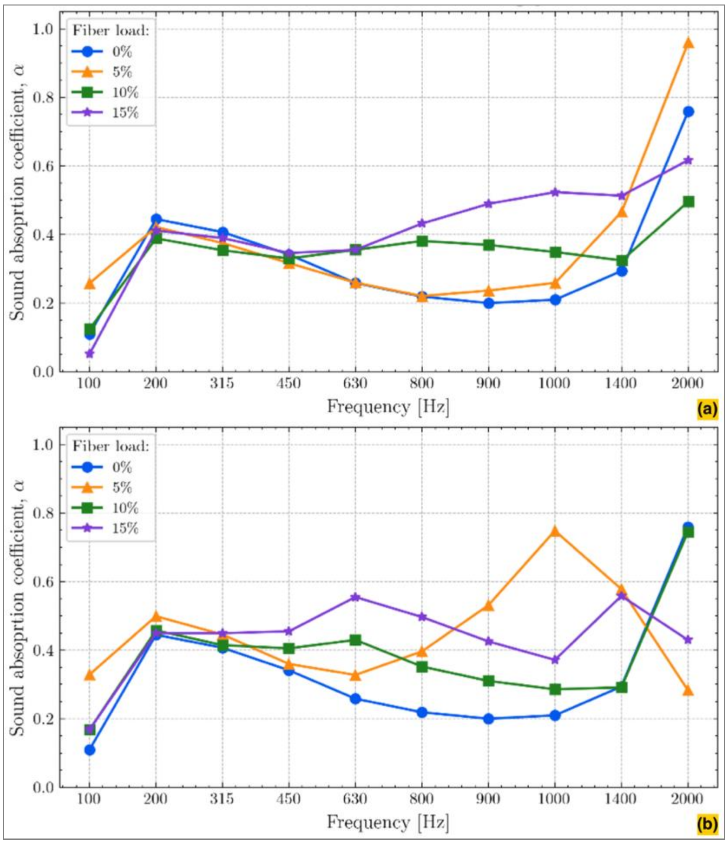

Figure 8. Sound absorption coefficient: (a) Without airgap; (b) With 10 mm air gap

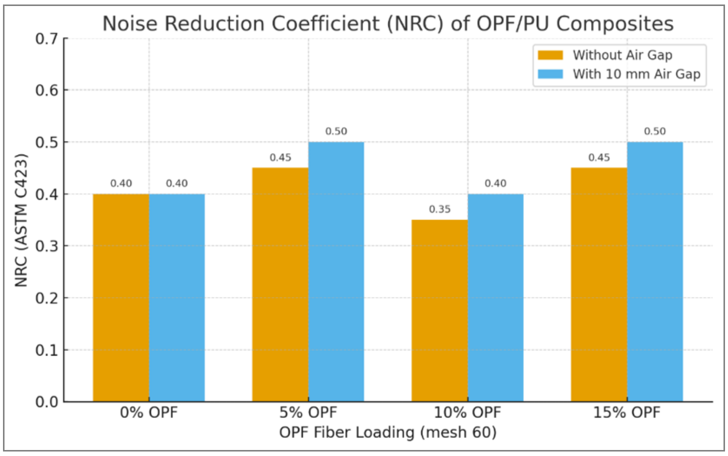

Figure 9. Noise Reduction Coefficient (NRC) of OPF/PU composites

bands [26], [27], [29]. Comparable results have been reported in other cavity-backed bio-composites, where combining porous resistive layers with air gaps consistently enhances mid-frequency absorption [26], [30], [31].

Overall, these findings highlight that fiber loading and air gap configuration must be co-optimized. While low fiber content (5 wt%) is particularly effective for high-frequency absorption, higher loading (15 wt%) becomes advantageous when combined with a backing cavity, broadening absorption into the low–mid frequency range. higher loading (15 wt%) becomes advantageous when combined with a backing cavity, broadening absorption into the mid-frequency range (400–1600 Hz). This interplay confirms that PU/OPF composites can be tailored as sustainable sound absorbers by balancing fiber dispersion, matrix adhesion, and structural design.

The findings of this study reveal a distinct trade-off between the structural integrity and acoustic functionality of the OPF-PU composites. While the Noise Reduction Coefficient (NRC) improved from 0.40 to 0.50 (with a 10 mm air gap), the maximum compressive stress experienced a systematic reduction of approximately 47% (dropping from 0.19 N/mm² to 0.094 N/mm²). This inverse relationship suggests a 'favorable compromise' where the refinement of the pore network and increased tortuosity which are essential for acoustic energy dissipation simultaneously act as structural diluents that weaken the load-bearing capacity. Consequently, these composite foams are not intended for primary structural applications. Instead, they are specifically designed for non-load-bearing applications, such as eco-friendly acoustic panels for building interiors, automotive door liners, and industrial insulation where lightweight, sustainable, and broadband noise-control properties are the priority over high compressive resistance.

4. Conclusion

This work demonstrates that incorporating oil palm frond (OPF) fibers into polyurethane foams establishes a clear structure–property–performance relationship. Increasing fiber content refines pore morphology and promotes tougher fracture paths, but also reduces compressive strength due to higher slurry viscosity, agglomeration, and limited interfacial bonding. The findings highlight OPF fibers as a promising renewable reinforcement for multifunctional performance. While they lead to a moderate reduction in mechanical strength, their ability to refine pore morphology and establish tougher fracture paths allows them to be strategically tuned for either lightweight structural components with added damping or for high-performance broadband acoustic insulation panels. These results indicate that for applications requiring higher structural integrity, future work should explore surface treatments to overcome the natural hydrophilic-hydrophobic mismatch observed in this study. From an acoustic standpoint, low fiber loading (5 wt%) produced superior high-frequency absorption, while higher loading (15 wt%) combined with an air gap broadened performance into the mid-frequency range; in contrast, 10 wt% composites consistently underperformed due to poor dispersion. Together, these findings reveal that OPF fibers can be strategically tuned to design eco-friendly foams tailored either for lightweight structural components with added damping or for broadband acoustic insulation panels, marking a step forward in the sustainable use of agricultural byproducts for advanced material applications.

Acknowledgements

The authors gratefully acknowledge the support of the Directorate General of Higher Education, Research, and Technology (DIKTI), Ministry of Higher Education, Science, and Technology of the Republic of Indonesia, for funding this research through the PFR Research Grant No. 138/C3/DT.05.00/PL/2025; 005/LL17/DT.05.00/PL/2025; 08/PRJ/II.3.AU/F/7/2025. The authors also thank the laboratory staff and colleagues at Fakulti Teknologi dan Kejuruteraan

Industri dan Pembuatan (FTKIP), Universiti Teknikal Malaysia Melaka for their assistance with experimental work and characterization, as well as the students whose contributions during material preparation and testing helped bring this study to completion.

Authors' Declaration

Authors' contributions and responsibilities – Conceptualization, B.I and J.A.R.; Methodology, B.I.; A and J.A.R.; Validation, B.I. and J.A.R.; Formal analysis, B.I.; A. and C.M.; Investigation, B.I.; A. and C.M.; Resources, B.I. and J.A.R.; Data curation, B.I. and A.; Writing—original draft preparation, B.I.; Writing—review and editing, B.I. and J.A.R. All authors have read and agreed to the published.

Funding – This research was funded by the Directorate General of Higher Education, Research, and Technology (DIKTI), Ministry of Education, Culture, Research, and Technology of the Republic of Indonesia, under the Research Grant No. 138/C3/DT.05.00/PL/2025; 005/LL17/DT.05.00/PL/2025; 08/PRJ/II.3.AU/F/7/2025.

Availability of data and materials – The data supporting the findings of this study are available from the corresponding author upon reasonable request.

Competing interests – The authors declare no competing interests.

Generative AI statement – During the preparation of this manuscript, the authors used generative artificial intelligence tools for language editing and proofreading purposes only. The authors reviewed and edited the content and take full responsibility for the content of the published manuscript.

Additional information – No additional information from the authors.

References

[1] Y. Fu and X. Wang, "Advancements and trends in vehicle sound package for noise control: A comprehensive review," *Advances in Mechanical Engineering*, vol. 17, no. 6, Jun. 2025, doi: 10.1177/16878132251345867.

[2] B. Mohammadi, A. Safaiyan, P. Habibi, and G. Moradi, "Evaluation of the acoustic performance of polyurethane foams embedded with rock wool fibers at low-frequency range; design and construction," *Applied Acoustics*, vol. 182, p. 108223, Nov. 2021, doi: 10.1016/j.apacoust.2021.108223.

[3] M. Liang, H. Wu, J. Liu, Y. Shen, and G. Wu, "Improved sound absorption performance of synthetic fiber materials for industrial noise reduction: a review," *Journal of Porous Materials*, vol. 29, no. 3, pp. 869–892, Jun. 2022, doi: 10.1007/s10934-022-01219-z.

[4] S. Dong *et al.*, "Recent Advances in Preparation and Structure of Polyurethane Porous Materials for Sound Absorbing Application," *Macromolecular Rapid Communications*, vol. 45, no. 14, Jul. 2024, doi: 10.1002/marc.202400108.

[5] N. Rastegar, A. Ershad-Langroudi, H. Parsimehr, and G. Moradi, "Sound-absorbing porous materials: a review on polyurethane-based foams," *Iranian Polymer Journal*, vol. 31, no. 1, pp. 83–105, Jan. 2022, doi: 10.1007/s13726-021-01006-8.

[6] X. Zhao, Y. Liu, Y. Lv, and M. Liu, "Research on lignin-modified flexible polyurethane foam and its application in sound absorption," *Journal of Industrial and Engineering Chemistry*, vol. 137, pp. 327–337, Sep. 2024, doi: 10.1016/j.jiec.2024.03.019.

[7] A. Korjakins, G. Sahmenko, and V. Lapkovskis, "A Short Review of Recent Innovations in Acoustic Materials and Panel Design: Emphasizing Wood Composites for Enhanced Performance and Sustainability," *Applied Sciences*, vol. 15, no. 9, p. 4644, Apr. 2025, doi: 10.3390/app15094644.

[8] M. Amran, R. Fediuk, G. Murali, N. Vatin, and A. Al-Fakih, "Sound-Absorbing Acoustic Concretes: A Review," *Sustainability*, vol. 13, no. 19, p. 10712, Sep. 2021, doi: 10.3390/su131910712.

[9] M. Zieleniewska *et al.*, "Development and applicational evaluation of the rigid polyurethane foam composites with egg shell waste," *Polymer Degradation and Stability*, vol. 132, pp. 78–86, Oct. 2016, doi: 10.1016/j.polymdegradstab.2016.02.030.

[10] H. Olcay and E. D. Kocak, “Rice plant waste reinforced polyurethane composites for use as the acoustic absorption material,” *Applied Acoustics*, vol. 173, p. 107733, Feb. 2021, doi: 10.1016/j.apacoust.2020.107733.

[11] J. Andersons, M. Kirpluks, and U. Cabulis, “Reinforcement Efficiency of Cellulose Microfibers for the Tensile Stiffness and Strength of Rigid Low-Density Polyurethane Foams,” *Materials*, vol. 13, no. 12, p. 2725, Jun. 2020, doi: 10.3390/ma13122725.

[12] S. B. Murmu, “Alternatives derived from renewable natural fibre to replace conventional polyurethane rigid foam insulation,” *Cleaner Engineering and Technology*, vol. 8, p. 100513, Jun. 2022, doi: 10.1016/j.clet.2022.100513.

[13] T. Yang *et al.*, “Sound Absorption Properties of Natural Fibers: A Review,” *Sustainability*, vol. 12, no. 20, p. 8477, Oct. 2020, doi: 10.3390/su12208477.

[14] L. K. Lazzari, E. F. Kerche, F. R. Figueiredo, R. F. C. de Albuquerque, B. Bortoli, and R. D. O. Polkowski, “Polyurethane foam coated with organic filers for sound absorption: A briefre view,” in *SAE Technical Paper*, Jan. 2024. doi: 10.4271/2023-36-0088.

[15] L. F. Ng *et al.*, “Mechanical Characterization, Water Absorption, and Thickness Swelling of Lightweight Pineapple Leaf/Ramie Fabric-Reinforced Polypropylene Hybrid Composites,” *Polymers*, vol. 16, no. 13, p. 1847, Jun. 2024, doi: 10.3390/polym16131847.

[16] R. Kovuru and J. Schuster, “Enhancing Mechanical Properties of Hemp and Sisal Fiber-Reinforced Composites Through Alkali and Fungal Treatments for Sustainable Applications,” *Journal of Manufacturing and Materials Processing*, vol. 9, no. 6, p. 191, Jun. 2025, doi: 10.3390/jmmp9060191.

[17] C. Kuranchie, A. Yaya, and Y. D. Bensah, “The effect of natural fibre reinforcement on polyurethane composite foams – A review,” *Scientific African*, vol. 11, p. e00722, Mar. 2021, doi: 10.1016/j.sciaf.2021.e00722.

[18] C. Patil, R. Ghorpade, and R. Askhedkar, “Investigation into the sound absorptivity of perforated panels with tapered hole geometries coupled with polyurethane foam,” *International Journal on Interactive Design and Manufacturing (IJIDeM)*, vol. 19, no. 3, pp. 1849–1868, Mar. 2025, doi: 10.1007/s12008-024-01864-5.

[19] S. Ekbatani, P. Rattanawongkun, S. Klayya, D. G. Papageorgiou, N. Soykeabkaew, and H. Zhang, “Hierarchical Natural Fibre Composites Based on Cellulose Nanocrystal-Modified Luffa Structures for Binderless Acoustic Panels,” *Polymers*, vol. 17, no. 3, p. 281, Jan. 2025, doi: 10.3390/polym17030281.

[20] S. Khem, Sutikno, P. Suwarta, and B. Istana, “Experimental Study of Sound Absorption Coefficient Characteristics of Oil Palm Frond Reinforced Composite,” *Key Engineering Materials*, vol. 941, pp. 257–263, Mar. 2023, doi: 10.4028/p-5t05f8.

[21] M. Mohammadi, M. R. Ishak, M. T. H. Sultan, and E. S. Zainudin, “A Comprehensive Review of Factors Influencing the Sound Absorption Properties of Micro-Perforated Panel Structures,” *Journal of Vibration Engineering & Technologies*, vol. 13, no. 5, p. 319, Jun. 2025, doi: 10.1007/s42417-025-01849-y.

[22] M. Y. Khalid, A. Al Rashid, Z. U. Arif, W. Ahmed, H. Arshad, and A. A. Zaidi, “Natural fiber reinforced composites: Sustainable materials for emerging applications,” *Results in Engineering*, vol. 11, p. 100263, Sep. 2021, doi: 10.1016/j.rineng.2021.100263.

[23] V. K. Singh and S. Mukhopadhyay, “Banana fibre-based structures for acoustic insulation and absorption,” *Journal of Industrial Textiles*, vol. 51, no. 9, pp. 1355–1375, Apr. 2022, doi: 10.1177/1528083720901823.

[24] M. Y. Yuhazri, B. Paramananthan, M. H. Amirhafizan, and H. Sihombing, “Coconut fiber panel towards acoustical performance,” *International Journal of Mechanical and Mechatronics Engineering*, vol. 19, no. 2, pp. 11–24, 2019.

[25] I. Wadgave, S. Kulkarni, S. Katekar, and M. Kulkarni, “A comprehensive review on: Mechanical and acoustical characterization of natural fiber-reinforced composite,” *Materials Today: Proceedings*, May 2024, doi: 10.1016/j.matpr.2024.05.002.

[26] L. Qi *et al.*, “Highly efficient acoustic absorber designed by backing cavity-like and filled-microperforated plate-like structure,” *Materials & Design*, vol. 225, p. 111484, Jan. 2023, doi: 10.1016/j.matdes.2022.111484.

[27] A. Y. Ismail, M. R. Omar, M. A. Anuar Hashim, and M. R. Md Radzi, “Improved Sound

Absorption Performance of Nonwoven Fabric using Fabric Facing and Air Back Cavity," *MATEC Web of Conferences*, vol. 97, p. 01086, Feb. 2017, doi: 10.1051/matecconf/20179701086.

[28] T. Koizumi, N. Tsujiuchi, and A. Adachi, "The Development Of Sound Absorbing Materials Using Natural Bamboo Fibers," in *High Performance Structures and Composites*, 2002, pp. 157–166. doi: 10.2495/HPS020161.

[29] H. Qui and Y. Enhui, "Effect of Thickness, Density and Cavity Depth on the Sound Absorption Properties of Wool Boards," *Autex Research Journal*, vol. 18, no. 2, pp. 203–208, Jun. 2018, doi: 10.1515/aut-2017-0020.

[30] R. Del Rey, A. Uris, J. Alba, and P. Candelas, "Characterization of Sheep Wool as a Sustainable Material for Acoustic Applications," *Materials*, vol. 10, no. 11, p. 1277, Nov. 2017, doi: 10.3390/ma10111277.

[31] T. Hassan *et al.*, "Factors Affecting Acoustic Properties of Natural-Fiber-Based Materials and Composites: A Review," *Textiles*, vol. 1, no. 1, pp. 55–85, 2021, doi: 10.3390/textiles1010005.